Supplementary materials

Decoupled electrolytes towards enhanced energy and high temperature performance of thermally regenerative ammonia batteries

Weiguang Wang[a,b], Gequn Shu[a], Xiuping Zhu[c], Hua Tian[a,*]

a: State Key Laboratory of Engines, Tianjin University, Tianjin, 300072, China

b: Program of Materials Science and Engineering, Department of Applied Physics and Applied Mathematics, Columbia University, New York, 10027, United States

c: Department of Civil and Environmental Engineering, Louisiana State University, Baton Rouge, LA 70803, United States

*: Corresponding author:

Dr. Hua Tian: thtju@tju.edu.cn, +86-15822683137

Calculations for the anode and cathode coulombic efficiency during charge and discharge:

In the discharge cycle:

$$CCE_d = \frac{(m_{f,Cu} - m_{0,Cu})\, n\, F}{C_d\, M_{Cu}} \times 100$$

$$ACE_d = \frac{C_d\, M_{Zn}}{(m_{0,Zn} - m_{f,Zn})\, n\, F} \times 100 \quad \text{(S1)}$$

In the charge cycle:

$$CCE_c = \frac{(m_{f,Zn} - m_{0,Zn})\, n\, F}{C_c\, M_{Zn}} \times 100$$

$$ACE_c = \frac{C_c M_{Cu}}{(m_{0,Cu} - m_{f,Cu}) n F} \times 100 \quad \text{(S2)}$$

where m_0 and m_f denote the electrode masses before and after the discharge or charge tests, F is the Faraday constant of 96485 C mol^{-1}, n is the number of electron involved in the electrode reaction (n = 2 for Cu and Zn), C_d and C_c are the total charge transferred and subscripts *d* and *c* represent the discharge and charge processes, respectively, and M_{Cu} and M_{Zn} are the molecular weight of the metals (Cu, 63.55 g mol^{-1}; Zn, 65.38 g mol^{-1}).

Table S1 The electrolyte pH in each chamber of traditional and decoupled Cu/Zn-TRABs with double-AEM design before and after constant current discharging under different conditions (the pH before discharging is identical due to the same used electrolytes).

pH Before or after discharging		Catholyte (0.1 M Cu(II) and 1 M $(NH_4)_2SO_4$)	Middle layer (1 M or 3 M $(NH_4)_2SO_4$)	Anolyte (0.1 M Zn(II), 1 M $(NH_4)_2SO_4$ and 2 M NH_3)
Before reaction		3.82	5.47 or 5.31	10.29
After discharging	0mm	8.9	-	9.91
	1mm with 3 M $(NH_4)_2SO_4$	7.97	9.26	9.95
	5mm with 3 M $(NH_4)_2SO_4$	7.44	9	9.99
	5mm with 1 M $(NH_4)_2SO_4$	7.91	9.46	9.86

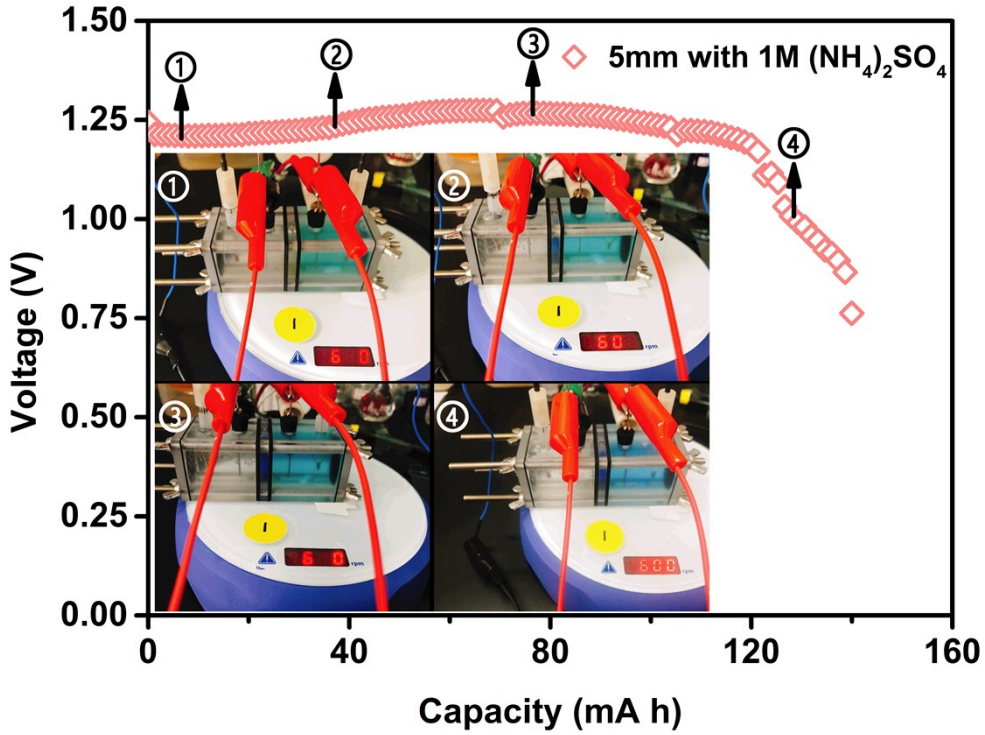

Fig. S1. Discharge voltage of a decoupled Cu/Zn-TRAB (P-AMV-AMV-N) with 5 mm thickness central chamber and 1 M $(NH_4)_2SO_4$. The inserted graphs show the color changes of catholyte and buffer electrolyte in the central chamber. The catholyte changes from light blue (Cu^{2+}, figure ①, ②, and ③) to dark blue ($Cu(NH_3)_4^{2+}$, figure ④), which demonstrates that the transition of main cathodic reaction is the direct cause of the decline in battery performance. The buffer electrolyte in the central chamber is colorless at first (figure ①), and soon turns dark blue (figure ②), then the color keeps getting dark (figure ③ and ④), indicating the existence of self-discharge phenomenon.

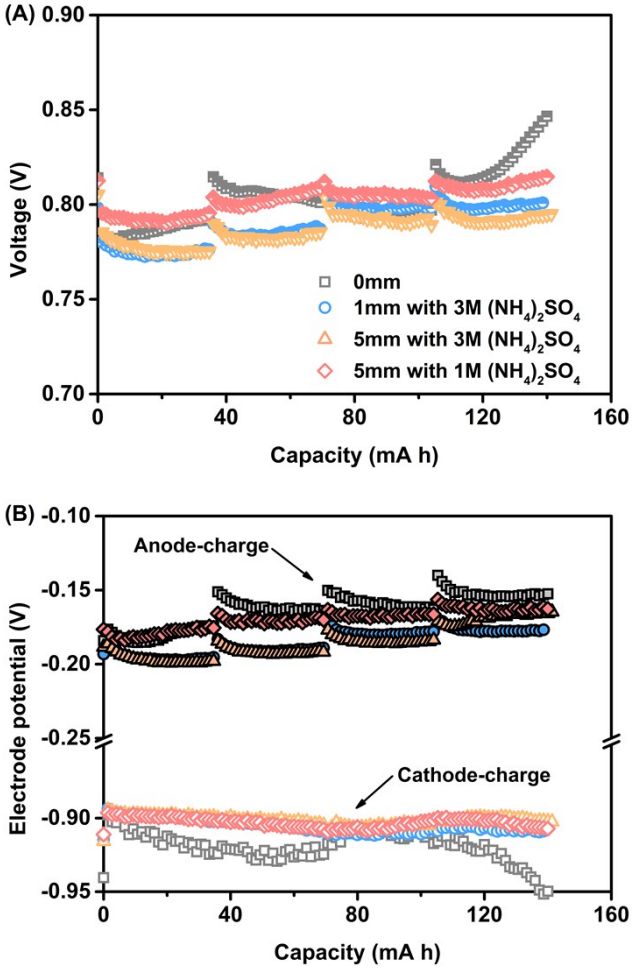

Fig. S2. Enlarge drawings of (A) charge voltage and (B) electrode potentials generated in one cycle by traditional and decoupled Cu/Zn-TRABs with different thicknesses and $(NH_4)_2SO_4$ concentrations of central layers.

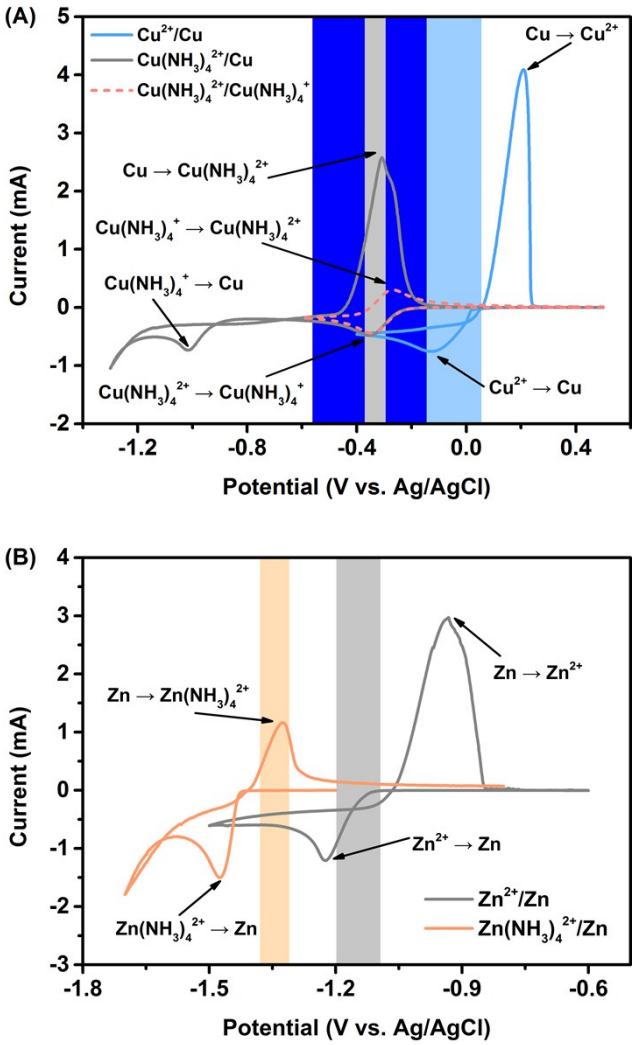

Fig. S3. (A) CV curves (scan rate of 10 mV s^{-1}) obtained with the catholyte (0.1 M $CuSO_4$ and 1 M $(NH_4)_2SO_4$) during discharge and the anolyte (0.1 M $CuSO_4$, 1 M $(NH_4)_2SO_4$ and 2 M $NH_3 \cdot H_2O$) during charge at a glassy carbon rotating disk electrode. The highlighted light blue area shows the cathode potential range before the tradition area during discharge ($Cu^{2+} \rightarrow Cu$), and the dark blue area represents the cathode potential range after the tradition area during discharge ($Cu(NH_3)_4^{2+} \rightarrow Cu$). The highlighted gray area denotes the anode potential range during charge

($Cu \rightarrow Cu(NH_3)_4^{2+}$). (B) CV curves (scan rate of 10 mV s^{-1}) obtained with the catholyte (0.1 M $ZnSO_4$ and 1 M $(NH_4)_2SO_4$) during charge and the anolyte (0.1 M $ZnSO_4$, 1 M $(NH_4)_2SO_4$ and 2 M $NH_3 \cdot H_2O$) during discharge at a glassy carbon rotating disk electrode. The highlighted gray area shows the cathode potential range during charge ($Zn^{2+} \rightarrow Zn$), and the orange area indicates the anode potential range during discharge ($Zn \rightarrow Zn(NH_3)_4^{2+}$).

Table S2 The electrolyte pH in each chamber of traditional and decoupled Cu/Zn-TRABs with double-AEM design before and after constant current charging under different conditions (the catholyte and anolyte pH before charging is determined by thermal regeneration process).

pH / Before or after charging		Catholyte (0.1 M Zn(II) and 1 M $(NH_4)_2SO_4$)	Middle layer (1 M or 3 M $(NH_4)_2SO_4$)	Anolyte (0.1 M Cu(II), 1 M $(NH_4)_2SO_4$ and 2 M NH_3)
0 mm	Before	6.73	-	10.36
	After	8.15	-	10.1
1mm with 3 M $(NH_4)_2SO_4$	Before	6.73	5.31	10.28
	After	7.56	9.57	10.2
5mm with 3 M $(NH_4)_2SO_4$	Before	6.75	5.31	10.3
	After	7.42	9.13	10.17
5mm with 1 M $(NH_4)_2SO_4$	Before	6.87	5.47	10.2
	After	7.53	9.54	10.15

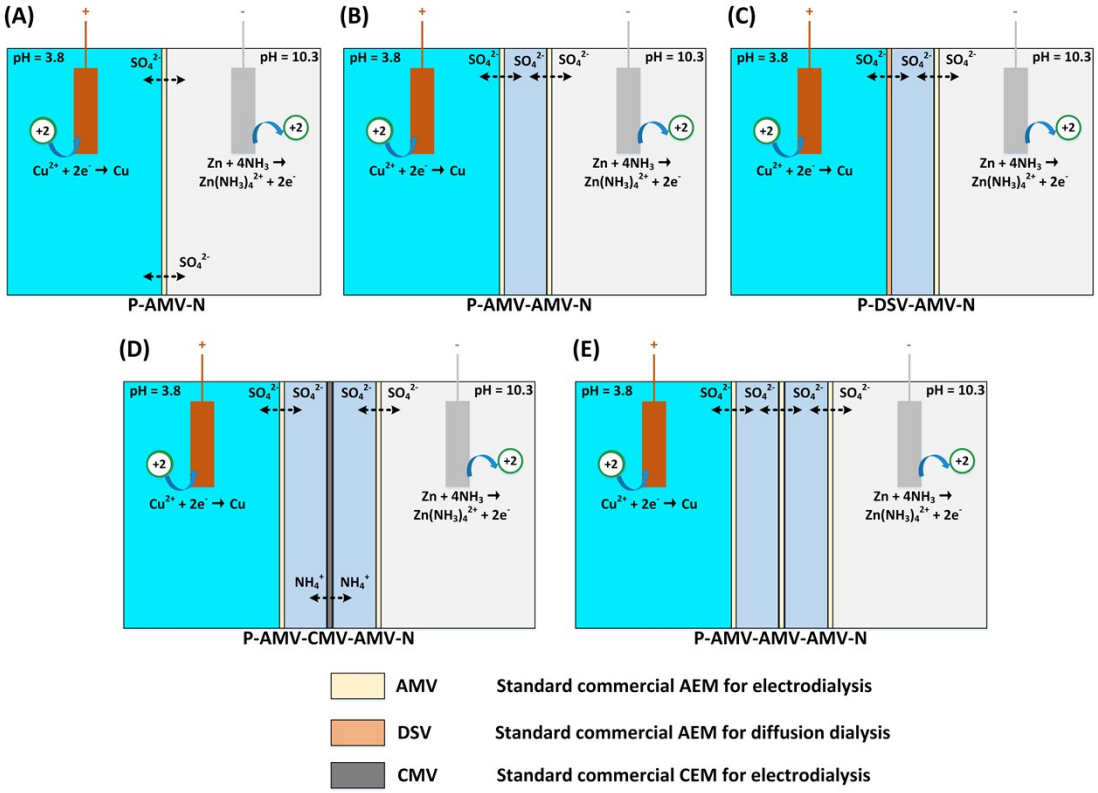

Fig. S4. Five decoupled Cu/Zn-TRABs with various designs (single-IEM system: (A) P-AMV-N; double-IEM system: (B) P-AMV-AMV-N and (C) P-DSV-AMV-N; triple-IEM system: (D) P-AMV-CMV-AMV-N and (E) P-AMV-AMV-AMV-N; P and N denote the positive and negative electrodes, respectively). DSV and AMV are both anion exchange membranes (AEMs), but compared to AMV, DSV has a smaller membrane resistance, but has poor selectivity. The AEMs (AMV and DSV) and CEM (CMV) mainly allow the transfer of SO_4^{2-} and NH_4^+, respectively.

Table S3 The electrolyte pH in each chamber of traditional single-IEM and decoupled Cu/Zn-TRABs with double and triple-IEM designs before and after constant current discharging (the pH before discharging is identical due to the same used electrolytes).

pH / Before or after discharging		Catholyte (0.1 M Cu(II) and 1 M $(NH_4)_2SO_4$)	1 mm Middle layer with 3 M $(NH_4)_2SO_4$)		Anolyte (0.1 M Zn(II), 1 M $(NH_4)_2SO_4$ and 2 M NH_3)
Before discharging		3.82	5.31		10.29
After discharging	P-AMV-N	8.9	-		9.91
	P-AMV-AMV-N	7.97	9.26		9.95
	P-DSV-AMV-N	8.39	8.98		9.95
	P-AMV-CMV-AMV-N	7.58	9.24	9.36	9.87
	P-AMV-AMV-AMV-N	7.26	9.06	9.47	9.88

Table S4 The electrolyte pH in each chamber of traditional single-IEM and decoupled Cu/Zn-TRABs with double and triple-IEM designs before and after constant resistance discharging (the pH before discharging is identical due to the same used electrolytes).

pH / Before or after discharging		Catholyte (0.1 M Cu(II) and 1 M $(NH_4)_2SO_4$)	1 mm Middle layer with 3 M $(NH_4)_2SO_4$)		Anolyte (0.1 M Zn(II), 1 M $(NH_4)_2SO_4$ and 2 M NH_3)
Before discharging		3.82	5.31		10.29
After discharging	P-AMV-N 10Ω	6.08	-		10.00
	P-AMV-AMV-N 14Ω	5.09	9.22		10.03
	P-AMV-AMV-AMV-N 15Ω	4.64	8.48	9.34	9.91

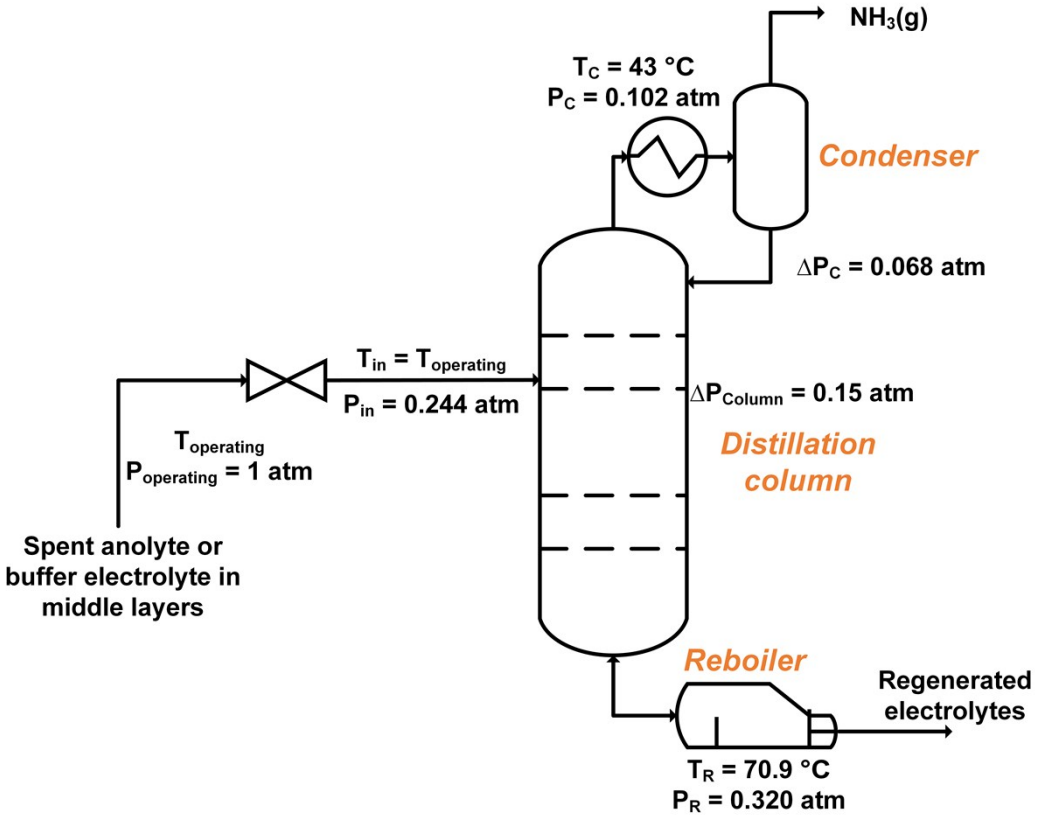

Fig. S5. A distillation column model for ammonia separation from the spent anolyte and buffer solution based on Aspen HYSYS. After the discharge or charge process, the pH of buffer solution in middle layers increases to 9 ~ 9.6 from 5.3, so these electrolytes also need to be regenerated.

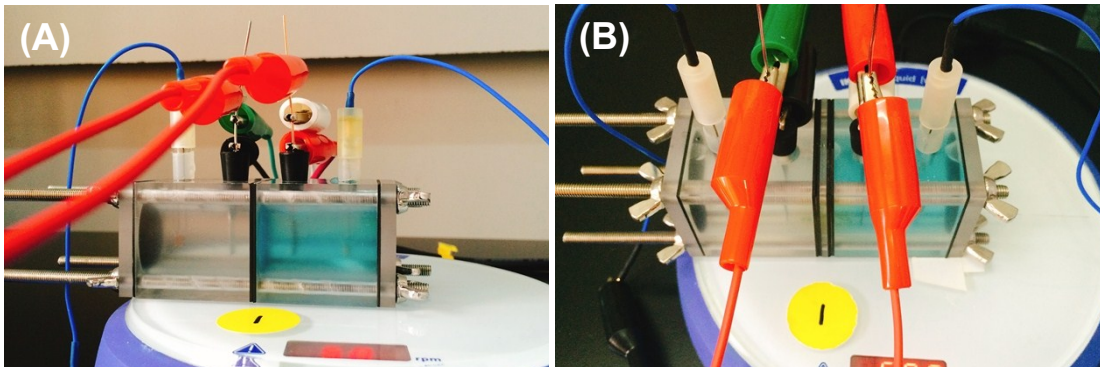

Fig. S6. Testing setup of (A) the traditional and (B) the decoupled Cu/Zn-TRAB.

Table S5 The recorded electrode potentials (E_{test}) are relative to the Ag/AgCl reference electrode ($E_{Ag/AgCl}$), and the reported potentials in this work are standard hydrogen electrode potentials and determined by $E_{test} + E_{Ag/AgCl}$. At different temperatures (T = 10 ~ 70 °C), the potentials of the Ag/AgCl reference electrode with 3.5 M KCl are calculated by Nernst equation of $E_{Ag/AgCl,T} = E_{Ag/AgCl,T}^{\theta} - (RT/F)\ln(a_{Cl^-,T})$, where $E_{Ag/AgCl,T}^{\theta} = E_{Ag/AgCl,298}^{\theta} + (T-298.15)(dE^{\theta}/dT)_{298}$ (T in K) $\approx 0.23659 - 4.8564 \times 10^{-4}\ T - 3.4205 \times 10^{-6}\ T^2 - 5.869 \times 10^{-9}\ T^3$ (T in °C), $a_{Cl^-,T}$ is the activity of Cl^- at the temperature of T and estimated by Visual MINTEQ software with SIT model. Room temperature is closed to 25 °C.

Temperature (°C) / Potential (V)	10	20	25	30	40	50	60	70
$E_{Ag/AgCl,T}$	0.2146	0.2083	0.2049	0.2013	0.1935	0.1850	0.1756	0.1654